Belantamab Mafodotin Triggers Immune Invigoration in Multiple Myeloma Via Inflammatory and Immunogenic Cell Death

Short title: Belantamab mafodotin triggers immune invigoration

Edmund CR Watson,[1,2] Halima Ali Shuwa,[3] Morgan Heycock,[3] Jenny Wade,[3] Chen-Yi Wang,[1,2] Mint Htun,[3] Lingzi Li,[4] Vivianne Niehaus,[4,5] Warren Baker,[1,2] Benjamin Miller,[3] Ruben M Drews,[3] Paul R Barber,[3] Yinjiao Ma,[6] Diana Munera,[3] Qingqing Hong,[6] Daniel E. Lowther,[3] Ali Cenk Aksu,[1] Lydia Lee,[7] H. Christian Eberl,[4] Eleanor Calcutt,[1,2] Sarah Gooding,[2,8] Yuqi Shen,[8] Abdullah Khan,[8] Joanna Hester,[9] Fadi Issa,[9] Giorgio Napolitani,[3] Hanny Musa,[10] Karthik Ramasamy,[1,2] Udo Oppermann,*[1,2] and Sue Griffin*[3]

*Equal contributions

[1]Botnar Research Centre, NIHR BRC Oxford, Nuffield Department of Orthopaedics, Rheumatology and Musculoskeletal Sciences, University of Oxford, OX3 7LD, UK

[2]Oxford Translational Myeloma Centre, University of Oxford, OX3 7LD, UK

[3]GSK, Stevenage, UK SG1 2NY

[4]GSK, Heidelberg, Germany, 69117

[5]Genomics Core facility, EMBL Heidelberg, Germany, 69117

[6]GSK, Collegeville, USA, 19426

[7]University College London, London, UK WC1E 6BT

[8]Medical Research Council (MRC) Molecular Haematology Unit, Weatherall Institute of Molecular Medicine, University of Oxford, OX3 9DS, UK

[9]Nuffield Department of Surgical Sciences, University of Oxford, OX3 9DU, UK

[10]GSK, Baar, Switzerland, 6340

ORCID IDs:

Watson ECR: 0000-0002-0950-9925

Shuwa HA: 0000-0002-7926-0360

Wang C-Y: 0000-0002-9710-8426

Li L: 0000-0002-6856-1299

Drews RM: 0000-0001-7360-4970

Aksu AC: 0000-0002-6525-3602

Eberl HC: 0000-0002-4159-5958

Gooding S: 0000-0002-1549-7043

Hester J: 0000-0002-7466-3849

Issa F: 0000-0002-8279-7732

Napolitani G: 0000-0002-3605-6394

Ramasamy K: 0000-0003-3385-3707

Oppermann U: 0000-0001-9984-5342

Griffin S: 0000-0002-8516-7787

Correspondence:

Udo Oppermann, email udo.oppermann@ndorms.ox.ac.uk

Botnar Research Centre, NIHR BRC Oxford, Nuffield Department of Orthopaedics, Rheumatology and Musculoskeletal Sciences, University of Oxford, OX3 7LD, UK;

Oxford Translational Myeloma Centre, University of Oxford, OX3 7LD, UK

Sue Griffin, email suzanne.a.griffin@gsk.com

GSK, Stevenage, UK SG1 2NY

Visual abstract

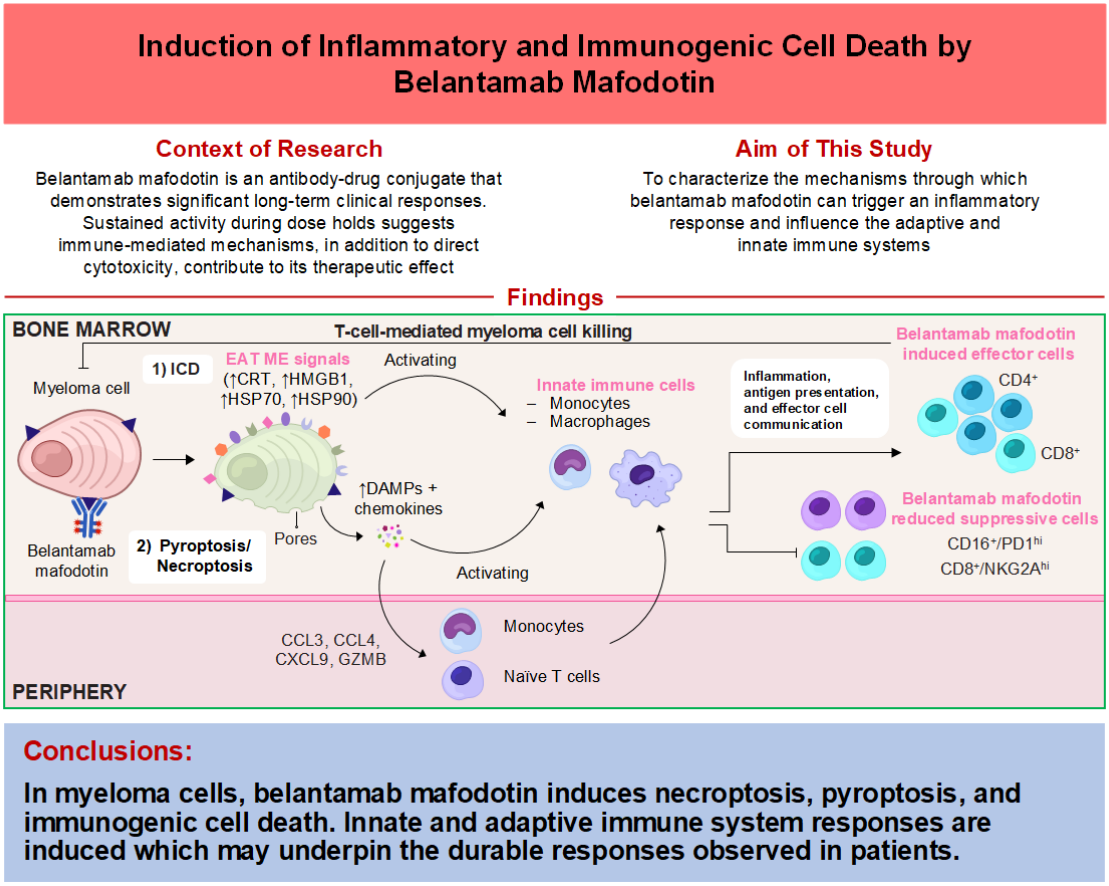

Conclusions:

In myeloma cells, belantamab mafodotin induces necroptosis, pyroptosis, and immunogenic cell death. Innate and adaptive immune system responses are induced which may underpin the durable responses observed in patients.

Key points

- Belantamab mafodotin induces immunogenic and inflammatory cell death to remodel the tumor microenvironment in patients
- Development of adaptive immunity may explain lasting effects seen in belantamab mafodotin-treated patients with RRMM

Abstract

Belantamab mafodotin, an antibody-drug conjugate targeting B-cell maturation antigen, has demonstrated significant clinical efficacy in combination therapies for relapsed or refractory multiple myeloma. Belantamab mafodotin exerts therapeutic effects through the cytotoxic action of its payload, monomethyl auristatin F, along with its ability to mediate antibody-induced cell death. Significant long-term clinical responses were previously observed in monotherapy treatment – even in patients undergoing dose holds – suggesting involvement of the adaptive immune system. Here, we show that belantamab mafodotin induces markers of immunogenic and inflammatory cell death *in vitro* and *ex vivo*. Belantamab mafodotin monotherapy treatment results in an acute inflammatory response that is detectable in patient serum within 24 hours, with increases in granzyme B, CXCL9, CCL3, and CCL4 linked to response depth. High expression of receptors LRP1 and TLR2 that mediate immunogenic cell death on patients' monocytoid (monocyte/macrophage) cells suggests an important function of the monocytoid lineage to mediate the observed inflammation and immunogenic cell death cascades. Inflammation is followed by remodeling of the innate and adaptive immune system, with a reduction in immune inhibitory signaling alongside the emergence of a CD4 granzyme B-expressing cell population in patients who are in remission vs those that relapse. The ability of belantamab mafodotin to promote adaptive immune responses in addition to its cytotoxic activity may help explain the durable responses observed in treated patients with relapsed/refractory multiple myeloma, despite dose and schedule modifications.

Introduction

Multiple myeloma (MM) is a cancer of bone marrow (BM)-resident plasma cells (PC), with patients typically experiencing a relapsing and remitting disease course.[1,2] The PC BM niche constitutes a tumor microenvironment (TME) densely populated with innate and adaptive immune cells in a complex stromal milieu. MM progression from precursor forms to clinically evident disease occurs alongside TME changes that support MM growth and persistence.[3]

Belantamab mafodotin comprises an afucosylated, humanized anti-B cell maturation antigen (BCMA) monoclonal IgGk1 linked to monomethyl auristatin F (MMAF), an anti-tubulin toxin payload.[4] The clinical efficacy of belantamab mafodotin monotherapy was initially demonstrated in late-line relapse, where despite modest overall response rates and median progression-free survival (PFS), robust and significant durations of response (DoR) were seen.[5,6] In phase 3 trials, belantamab mafodotin combinations achieved significant increases in PFS (DREAMM-7 [NCT04246047] and DREAMM-8 [NCT04484623]) and overall survival (OS) (DREAMM-7 [follow-up for DREAMM-8 ongoing]) versus standard-of-care triplets.[7,8] Dose and schedule modifications to manage ocular events were frequent.[5,6,9] Responding patients experienced more dose interruptions,[6] suggesting that clinical response continues in the absence of active treatment.

Preclinical studies suggest that belantamab mafodotin acts through a combination of natural killer (NK) cell recruitment to engage in antibody-dependent cellular cytotoxicity (ADCC); opsonization of PCs for antibody-dependent phagocytic cytotoxicity (ADCP); and cell death mediated directly by MMAF.[4,10,11] The latter leads to an immunogenic form of cell death that could trigger an adaptive immune response and immunologic memory.[4,10]

Immunogenic cell death (ICD) is a regulated cell death having three canonical signals: pre-apoptotic surface exposure of calreticulin, and the release of ATP and HMGB1 throughout cell death and post-mortem respectively.[12] Release of heat shock proteins and damage-associated molecular patterns (DAMPs) and other factors can accompany ICD.[13] These “eat me” and “find me” signals trigger dendritic cell (DC) activation via calreticulin and LRP1 (CD91) interaction on DCs,[13] which ultimately leads to T-cell-mediated immunologic memory against the tumor cells.[14] The evidence for belantamab mafodotin-associated ICD is derived from cell line data and a model of murine lymphoma overexpressing BCMA.[10]

While ICD is defined by the participation of an adaptive immune response, other forms of regulated cell death are characterized by inflammation alone and in some cases, can be triggered by tubulin stabilising toxins.[15,16] Pyroptosis and necroptosis exhibit release of inflammatory chemokines, cytokines, and

DAMPs through cell membrane pore formation, leading to local inflammation.[17] To delineate their activity from classic immunogenic cell death (ICD), we describe these 2 pathways as inflammatory cell death.[18,19]

We provide evidence that belantamab mafodotin triggers both inflammatory and immunogenic cell death in cell lines, *ex vivo* in samples from patients with MM and in patients treated with belantamab mafodotin. We suggest that belantamab mafodotin is associated with inflammation and immune priming in successfully treated patients, which contributes to the development of immunologic memory.

Methods

The studies referenced in this manuscript were conducted in accordance with the Declaration of Helsinki and Good Clinical Practice guidelines, and were approved by the relevant national, regional, or independent ethics committee or institutional review boards. All patients/donors provided written informed consent for use of their samples. Ethics committees overseeing the Oxford Radcliffe Biobank, HaemBio, and Oxford Musculoskeletal Biobank, all at the University of Oxford; the UCL Cancer Institute Biobank, at University College London; and the ProMMise trial, approved sample collection/use. Full details are in the **Supplemental Methods**.

Drug treatment of human MM cell lines (HMCLs) and BM mononuclear cells (BMMCs)

HMCLs or BMMCs were seeded into 96-well plates at 1×10^5 cells/well and incubated for 48 or 72 hours (HMCLs) or 16 hours (BMMCs) with indicated concentrations of belantamab mafodotin (GSK) or MMAF (Selleck Chem).

Flow cytometry

Briefly, HMCL or BMMCs were washed with phosphate-buffered saline (PBS) and resuspended in live/dead stain (1:400 dilution, Biolegend) and FcR block solution (1:100 dilution; Miltenyi) for 20 minutes before pelleting. Cells were stained with conjugated antibodies for 60 minutes, fixed, permeabilized, stained with intracellular antibodies for 60 minutes, followed by secondary antibodies for 40 minutes and acquired on a Cytek Aurora. In BMMC samples, viable MM BCMA+ cells were defined as CD45-CD40+BCMA+. Data were analyzed using FlowJo v10.10.0. Statistical analysis was performed in R 4.4.1. For each marker, a binomial proportions model was used and the Benjamini-Hochberg (BH) multiplicity correction was applied to control the false discovery rate (FDR) at 5%. Longitudinal

peripheral blood mononuclear cell (PBMC) samples from 33 patients in the ongoing DREAMM-5 (NCT04126200) study[20] were analyzed by flow cytometry using a TNBK immune cell phenotyping panel. Statistical analysis was performed using the Linear Mixed Model (LMM) to model the longitudinal data [lmer()] function from the lme4 package in R.

Bulk RNA sequencing

RNA was extracted using a KingFisher Apex system according to manufacturer's protocol and strand-specific bulk RNA sequencing conducted (RNAseq) (poly-A selection, Illumina 2×150 bp paired-end sequencing, 100 million reads). Differential gene expression analysis was performed using DESeq2.[21] Log2 fold changes between control and test agent were moderated using ashr.[22] Multiple testing correction was performed by controlling the FDR using Independent Hypothesis Weighting.[23]

Chemokine bioassay

Cell supernatant or serum from 43 patients from DREAMM-14 (NCT05064358) treated with belantamab mafodotin monotherapy were evaluated using a U-plex custom 10-plex kit (Mesoscale Discovery Platform; MSD) or HMGB1 ELISA (Cloud Clone) according to manufacturer's instructions. Concentrations were calculated using a standard curve for each analyte and corrected for dilution factor. Statistical analysis was performed in R version 4.4.1. For each secreted inflammatory mediator, a Linear Mixed or Bayesian Tobit model was implemented. Best confirmed response was used to determine response categories as outlined in **Supplemental Table 6**.

Proteomics

NCI-H929 (ATCC) supernatant was analyzed using Olink Explore 1536 according to manufacturer's instructions. Libraries were sequenced on a NovaSeq 6000 (Illumina). The lower limit of detection (LOD) provided by the NPX Explore software (v.3.9.0) was utilized for censoring. Statistical analyses were conducted using R version 4.3.1, with linear models fitted separately to each protein using the lm() function. P-values were adjusted for multiple testing using the Benjamini-Hochberg FDR method.

Multiplex immunofluorescence imaging

Twenty formalin-fixed paraffin-embedded trephine BM biopsies from 10 patients from DREAMM-5 sectioned to 4 µm were mounted on SuperFrost Ultra Plus™ GOLD Adhesion Slides (Epredia). Slides were baked, dewaxed, and treated with BOND Epitope Retrieval Solution 2 (Leica) using Leica BOND RX auto

stainer. Imaging was performed using the Leica Cell DIVE system through 7 rounds of fluorescent-label antibody staining, imaging, and dye inactivation with 3% hydrogen peroxide (Merck) and 0.1 M sodium bicarbonate (Merck). Image analysis used custom Python scripting. MM/PC were classified as CD138+BCMA+. Generalized least squares models were used to assess the percent cell type, density of cell type, or biomarker intensity change.

BM samples from belantamab mafodotin-monotherapy treated patients

BM aspirates acquired as part of routine care underwent CD138 negative selection (StemCell EasySep) and the CD138- fraction was separated on a Ficoll gradient and viably frozen.

Mass cytometry

Cells (3×10^6 per sample) were washed twice in Maxpar Cell Staining Buffer (CSB; Standard BioTools) and stained with pre-aliquoted surface and intracellular antibody cocktails (**Supplemental Table 5**). Data were acquired on a Helios mass cytometer (Standard Biotools), according to the manufacturer's protocol.

Single-cell transcriptomics

BM aspirate cells were processed using GEM-X beads (10X Genomics), with cDNA library amplification per the manufacturer's protocol (10X Genomics, user guide CG000731). cDNA libraries were quantified with TapeStation and 10 ng cDNA taken forward into the Oxford Nanopore (ONT) protocol using PCS114 chemistry on a Promethion P24 using R10.4.1 flow cells (ONT). Super-high accuracy basecalling was performed by Dorado within the MinKNOW software. FASTQ files were processed by running a singularity image of the wf-single-cell pipeline (EPI2ME) on a high-performance cluster, with the reference genome GRCh38 and expected cells set to 5000. Resulting transcript and counts matrices were imported into a Python environment and analyzed using a combination of scanpy,[24] SoupX,[25] scDblFinder,[26] and scVI.[27] Barcodes with counts and transcripts >5 median absolute deviations below the median and containing ≥20% mitochondrial genes were filtered.

Spatial transcriptomics

BM trephine sections (5 µm-thick) were assessed with a 480-gene custom Xenium panel (**Supplemental File 1**). Slides were processed on a 10X Xenium v1 platform (10X Genomics) including cell segmentation staining (10X Genomics, user guide CG000749, Rev A). Counts matrices and associated centroid and

segmentation coordinates were read into Seurat for R.[28] Following clustering and manual cell annotation, trephine data were tiled with 500 µm × 500 µm squares and clustered according to cell composition. CellChat analysis was performed to assess communication per tile.[29]

All statistical analyses for biomarker data was performed in a post-hoc, exploratory manner.

Results

Belantamab mafodotin response can persist through prolonged dose holds

In patients treated with belantamab mafodotin monotherapy as part of the named patient program, 3-month gaps between doses (where the labelled dosing schedule was once every 3 weeks) could be associated with ongoing remission **(Supplemental Figure 1)**, even with clinical responses of less than complete remission (CR). We hypothesized that ongoing responses in the absence of active treatment might be enabled by changes in the TME triggered by belantamab mafodotin treatment.

Belantamab mafodotin-mediated cell death triggers inflammatory and ICD pathways in MM cell lines and patient BM *ex vivo*

Mechanisms of belantamab mafodotin-induced cell death were characterized to better understand how belantamab mafodotin might influence the TME. Treatment of HMCLs with belantamab mafodotin triggered significant, dose-dependent, upregulation of "eat me" ICD markers (calreticulin, HMGB1, HSP70, and HSP90) on the cell surface **(Figure 1A and Supplemental Figure 2A)**. We also found dose-dependent expression of pore-forming proteins involved in the inflammatory cell death pathways, necroptosis (MLKL) and pyroptosis (GSDME and GSDMD) **(Figure 1A)**. These findings were recapitulated with free MMAF, indicating these pathways are induced by the antibody-drug conjugate's payload **(Figure 1B**). RNAseq of NCI-H929 cells after treatment with belantamab mafodotin, or free-MMAF, confirmed widespread transcriptional changes, including expression of genes associated with pyroptosis and necroptosis **(Figure 1C–D and Supplemental Figure 2B)**.

To validate these findings, we treated BM mononuclear cells (BMMCs) from 7 patients with MM *ex vivo* for 16 hours. Spectral flow cytometry analysis confirmed that belantamab mafodotin and MMAF induced significant upregulation of all tested markers in BCMA-positive PCs, indicating simultaneous induction of immunogenic and inflammatory pathways through the belantamab mafodotin payload **(Figure 1E-F and Supplemental Figure 2C).** BMMCs were treated with daratumumab as a negative control, which did not induce markers of ICD, necroptosis, or classical pyroptosis (GSDMD); GSDME increased, as expected,

since BMMCs contain NK cells, and GSDME expression can be triggered by NK cell killing via ADCC,[30] a known mechanism of daratumumab **(Supplemental Figure 2D)**.

Pyroptosis- and necroptosis-associated pores enable the release of inflammatory chemokines and cytokines. We used Olink-based proteomics to probe for proteins in the supernatant of NCI-H929 cells incubated with belantamab mafodotin and MMAF. From the 1432 measured proteins, over 100 were significantly elevated following 10 µg/mL belantamab mafodotin treatment, consistent with inflammatory cell death (**Figure 2A** and **Supplemental Figure 3A)**. Focusing on immune modulators, belantamab mafodotin and MMAF treatment resulted in accumulation of granzyme B (GZMB) and the proinflammatory mediators CXCL8 (IL8), CCL3, and CCL4, which are crucial for immune cell recruitment to inflamed tissues. GZMB is typically associated with cytotoxic T/NK cells; therefore, elevated secretion of this marker from MM cells in response to belantamab mafodotin was unexpected. However, all these factors are NF-kB response genes, which is a key downstream module of the necroptotic cell death pathway; additionally, GZMB cleaves GSDME, suggesting a potential interconnection between the necroptosis and pyroptosis pathways in belantamab mafodotin-treated cells **(Figure 2A).**

RNAseq of NCI-H929 cells showed significantly elevated levels of *GZMB*, *CXCL8*, *CCL3*, and *CCL4* following belantamab mafodotin and MMAF treatment, suggesting that the increase of chemokines can be attributed to transcriptional reprogramming to support the release of inflammatory mediators beyond simple cytosolic protein 'leakage' following cell necrosis **(Figure 2B and Supplemental Figure 3B)**. Using MSD, a high-sensitivity sandwich immunoassay, we additionally tested for previously reported pyroptosis and necroptosis-associated chemokines which were below the limit of detection in the proteomic analysis, and observed increases in CXCL1, IL16, IL18, and IL1β **(Figure 2C** and **Supplemental Figure 3C)**.

Investigating BMMCs from patients with MM treated *ex vivo* with belantamab mafodotin for 16 hours confirmed the release of CCL3, CCL4, CCL2, and CXCL9; other chemokines were not confirmed, likely due to shorter incubation time experienced by the primary cells **(Figure 2D)**. Treatment with free-MMAF did not lead to detectable chemokine secretion (data not shown), possibly due to excessive toxicity with primary cells, which was also noted in NCI-H929 cells, where treating with high MMAF concentrations led to lower chemokine secretion **(Supplemental Figure 3C).**

Together, these data support simultaneous activation of programmed cell death pathways that are immunogenic and inflammatory, triggering chemokine/cytokine release that could support the influx of immune cells into the BM.

Belantamab mafodotin monotherapy treatment induces a transient pro-inflammatory chemokine signature in peripheral blood of patients with MM

To study belantamab mafodotin-triggered inflammation in patients, we analyzed serum samples from 43 patients, collected at baseline, 24 hours post treatment, and 3 weeks post-dosing (prior to the second treatment cycle) with belantamab mafodotin monotherapy in the DREAMM-14 study.[31] Immunoassay analysis demonstrated significant spikes in pyroptosis- and necroptosis-related inflammatory factors 24 hours post first dose (**Figure 3A and 3B**). These included the ICD-associated DAMP, HMGB1, and inflammatory factors CCL2, CCL3, IL8, IL16, IL1β, CXCL9, GZMB, and CCL4, which returned toward baseline levels prior to the second cycle, highlighting the acute and transient nature of the belantamab mafodotin-triggered inflammatory response.

We used a linear mixed statistical model to evaluate if the longitudinal profile of these markers differed according to best clinical response achieved (time-by-response interaction). GZMB was significantly increased compared to baseline at 24 hours in patients who achieved deep response (≥ very good partial response) but not in non-responders, defined as progressive disease **(Figure 4)**. Additionally, CXCL9, CCL3, and CCL4 were identified through the time-by-response interaction assessment; these markers significantly increased at 24 hours in deep responders, but this increase was less pronounced in modest responders (i.e., those who achieved a partial response, minimal response, or stable disease) and non-responders. These findings indicate that successful induction of inflammatory mediators within 24 hours following treatment may trigger downstream events that support a deep therapy response.

The monocytoid population of the TME expresses receptors necessary for mediating ICD

To determine which TME components might receive and elaborate the inflammatory signal from dying PCs, single-cell RNAseq analysis was used to compare BM aspirates from 7 patients prior to treatment with belantamab mafodotin monotherapy (administered as part of the named patient program) with control BM samples from 4 age-matched patients (taken from femoral heads in patients undergoing elective hip arthroplasties for non-malignant disease) **(Supplemental Figure 1 and Figure 5A-B)**.

Baseline (pre-belantamab mafodotin initiation) samples demonstrated expanded T-lymphoid and NK cell compartments in patients with MM relative to non-malignant controls according to differential abundance analysis **(Figure 5B-C)**. Amongst the innate immune cells, the MM TME had fewer classical and plasmacytoid dendritic cells, more granulocytes, and in some cases, more monocytoid (monocyte/macrophage) cells. Classical DCs (cDCs) are canonical mediators of ICD, yet expression of pro-inflammatory ICD receptors *LRP1*, *TLR2*, *TLR4*, and *TREM1* was significantly greater in MM monocytoid

cells compared to cDCs. This appears to be an MM-specific observation, as no such (or less appreciable) differences were observed in control samples **(Figure 5D)**. Of interest, the inhibitory ICD receptor, TIM-3[32], encoded by *HAVCR2*, is much more highly expressed in cDCs than monocytoid cells, in both control and MM patients. *TLR2*, *TREM1*, *HAVCR2*, and *CXCR4* were differentially expressed in MM vs control monocytoid cells, suggesting MM-specific modulation of the monocytoid compartment **(Figure 5D)**.

We applied a 39-parameter mass cytometry immunophenotyping panel to the same samples. Differential abundance analysis of the baseline state by MiloR showed a non-significant increased representation of monocytoid populations but not cDC in responders compared to non-responders **(Figure 5E-F)**. Additionally, the observation that monocytoid chemokines (CCL3 and CCL4) transiently increase in the serum of patients who have deep therapy responses (**Figure 4**) indicates a potentially important contribution of this cell type to therapy response. Together, these data indicate monocytoid cells are the most likely myeloid population to be involved in relaying the immunogenic and inflammatory signal emitted by belantamab mafodotin-induced PC cell death.

Successful belantamab mafodotin treatment is associated with a reduction in immunosuppressive communication and the emergence of a key immune effector population

We sought changes in the TME that could represent sequelae of a belantamab mafodotin-triggered, monocytoid-amplified, acute inflammatory state. *In situ* spatial transcriptomics assessed cell–cell communication networks in matched baseline/remission samples from a responding patient, and additionally in a follow-up sample from a patient relapsing on treatment **(Figure 6A-B)**. PC proximity was controlled by tiling over each trephine and selecting tiles of approximately equal cell composition for comparison **(Supplemental Figure 4A)**. We found a reduction in the inhibitory signaling axes (*MIF* and *LGALS9)* from baseline to remission, with higher levels in relapse **(Figure 6B and Supplemental Figure 4B-D)**; the T- and NK-cell exhaustion marker, *TIGIT* showed a similar pattern **(Figure 6B)**. These communication changes from 2 patients were consistent with a broader trend of immune de-repression and invigoration seen across our mass cytometry dataset. Here, 5 responding patients had a larger, putatively inhibitory, CD16 and PDL1-double positive granulocyte population at baseline that diminished over time compared with the 2 non-responders **(Figure 6C and 6D)**.

Belantamab mafodotin-associated inflammation and immune de-repression may link to an emergent functional adaptive immune response. In the monotherapy cohort, the CD8 effector memory (CD8 EM)

compartment in the baseline BM was non-significantly expanded in responders compared to non-responders, and reduced in responding patients on treatment, while the CD4 central memory (CD4 CM) compartment appeared to expand **(Figure 6F and 6G)**. These observations were corroborated in an independent cohort of patients from the DREAMM-5 trial (a platform study assessing various belantamab mafodotin combination regimens), where we performed multiplex immunofluorescent imaging of BM trephines **(Supplemental Figure 5A–B)**. Here, there was an increase in the ICD marker HMGB1 and a trend towards expansion of CD4 and CD8 CM in responders with a decrease in CD4 and CD8 EM **(Supplemental Figure 5C–D)**. Aligned with the reduced inhibition concept, there was also reduction of an inhibitory (CD11b+) macrophage population in responders **(Supplemental Figure 5E)**. The observed loss of EM in the BM in both cohorts may indicate mobilization of functional EMs into the periphery: when we assessed the peripheral blood (PB) of a cohort of patients receiving belantamab mafodotin as part of DREAMM-5, we observed a significant increase in CD8 effector and CD8 EM in the periphery following treatment **(Supplemental Figure 6)**. Overall, these changes are consistent with the induction of adaptive immunity.

Deeper analysis of the adaptive immune compartment using the mass cytometry data described in Figure 5E-F, showed the emergence of a segregated CD4 GZMB-positive population over time in patients treated with belantamab mafodotin monotherapy **(Figures 6E-G).** At follow-up, this population was significantly more abundant in the remission than the relapse state **(Figure 6H)**. In this group of cells, GZMB levels were equivalent to the CD8 effector populations by normalized mass cytometry expression values (**Supplemental Figure 7)**, consistent with it being a *bona fide* cytotoxic, MHC-II-restricted effector group.

Collectively, we found changes in TME cellular architecture and communication that are consistent with activation of the adaptive immune system, and which correspond with successful belantamab mafodotin therapy.

Discussion

Enhanced understanding of belantamab mafodotin's mechanism of action may provide a mechanistic explanation of the robust efficacy observed across clinical trials, including the long-term DoR. Clinically, gaps of 3 months between doses of belantamab mafodotin monotherapy (where the labeled dosing

schedule was once every 3 weeks) could be associated with ongoing remission, even when response was less than CR. Concordant with this finding, a recent *post hoc* analysis of the phase 3 DREAMM-7 and DREAMM-8 trials showed sustained efficacy in patients despite extended dose delays.[33] We hypothesize that the occurrence of sustained clinical responses despite the absence of active treatment might be explained by a model where belantamab mafodotin-induced inflammatory death of PCs stimulates, and is amplified by, monocytoid cells, which then act as a crucial link in the de-repression and invigoration of the TME to induce durable therapeutic response that persists independent of the presence of drug.

Our results suggest that, in addition to ICD, belantamab mafodotin triggers inflammatory cell death by necroptosis and pyroptosis, which are forms of regulated cell death that release chemokines and DAMPs to trigger innate and adaptive immunity. We observed that the ICD marker HMGB1, alongside pyroptosis and necroptosis-associated inflammatory chemokines, increased in the peripheral serum of patients 24 hours after belantamab mafodotin treatment. In the case of HMGB1, this is consistent with prior findings,[34] while our inflammatory cell death findings represent a novel insight into MMAF's activity. Among the inflammatory chemokines, increases were seen in: CCL2, CCL3, CCL4, and IL8, which recruit and activate innate cells such as neutrophils and monocytes[35]; CXCL9 and IL16, which recruit T lymphocytes; and IL1β and IL18, which can enhance antigen-specific T-cell responses.[36] Accordingly, the cell death phenotype triggered by belantamab mafodotin provides an inflammatory milieu that could recruit an adaptive immune response.[37]

Our data support monocytoid cells as a primary interface relaying the PC death signal to an adaptive immune response. The greatest expression of ICD receptors LRP1 and TLR2 was seen in monocytoid cells; responders tended to have higher monocytoid cell numbers at baseline, and chemokines CCL3 and CCL4 (critical for monocytoid cells homing and activation) were elevated in the serum of patients who achieved a deep response. The homing of monocytoid populations after belantamab mafodotin treatmenthas also been demonstrated preclinically and may additionally support ADCP.[4] These findings suggest that constitution of the BM with a sufficient monocytoid population is necessary for the downstream immune cascade to enable a sustained response.

Remodeling of a polymorphonuclear myeloid-derived suppressor cell (PMN-MDSC) compartment might be an effector mechanism for changes in the TME. We saw a CD16- and PDL1-double positive cell population over-represented in responders vs non-responders at baseline, which receded with successful treatment. These cells expressed CD66b and CD11b, and segregated with low-density BMMCs on a Ficoll gradient, all characteristic of the PMN-MDSC phenotype, previously shown to be negatively

prognostic in MM.[38] The greater dominance of these cells in responders vs non-responders prior to therapy implies that belantamab mafodotin works best in TMEs that have the most to gain from de-repression. T-lymphoid compartment restructuring is another putative effector mechanism. Soluble GZMB and CXCL9 were released within 24 hours after belantamab mafodotin dosing and were linked to deep responses. Preclinical investigations indicated that GZMB may be released by MM cells undergoing belantamab mafodotin-induced inflammatory cell death, but since GZMB is a canonical marker of T- and NK-cell cytotoxicity, serum GZMB could also be derived from cytotoxic T-effector cells or NK cells that are activated through the inflammatory and immunogenic nature of MM cell death.

Consistent with this, we observed remodeling of the T-cell compartment and the emergence of a CD4 GZMB-positive population in responders, a cell type associated with a good prognosis in MM and other cancers.[39,40] These cells were less frequent in relapsing patients, suggesting they may hold important anti-MM potential. Given the lytic nature of PC death, the fact that these cells are MHC-II-restricted cytotoxic cells is particularly relevant. Tumor antigens from dying PCs subsequently presented by antigen-presenting cells, such as monocytes/macrophages, could enable the cytotoxic activity of CD4 T-cells against PCs (which express MHC-II).

In conclusion, patients treated with belantamab mafodotin exhibited an acute inflammatory phenotype after the first dose of therapy, which our *in vitro* data suggest is driven by inflammatory and immunogenic cell death. This led to release of inflammatory mediators detectable in patient serum, where CCL3, CCL4, CXCL9, and GZMB may act as early biomarkers of response. We propose that the recruitment of a monocytoid-dominated response to this inflammatory background leads to T-cell restructuring, emergence of a CD4 GZMB population, and loss of inhibitory cell types. The TME's ability to undergo this restructuring could be a key determinant of clinical response to belantamab mafodotin, and once restructured, the TME may be capable of controlling MM durably, even during dose holds.

Acknowledgements

EW was supported by Cancer Research UK (CRUK grant number SEBCATP-2022/100011). Research in the UO laboratory was supported through funding from GSK (UO, KR), Innovate UK, the National Institute for Health Research Oxford Biomedical Research Centre, Cancer Research UK, the Leducq Epigenetics of Atherosclerosis Network (LEAN) program grant from the Leducq Foundation, and the Myeloma Single Cell Consortium. SGo is supported by Cancer Research UK (CRUK grant number RCCCSF-Nov21\100004). Samples were obtained through HaemBio, the Oxford Radcliffe Biobank and the ProMMise trial team, and we acknowledge expert sample preparation support from Mirian Angulo Salazar, Batchimeg Usukhbayar, Vicki Gamble, Renuka Teague, and David Maldonado-Perez. We would like to acknowledge the advice of Tony Ng who provided the initial suggestion to explore inflammatory cell death as a potential mechanism of action and for reviewing the mechanistic aspects of the manuscript. We are grateful to Taryn Mockus-Daehn for support with flow cytometry panel design and analysis, Aurelie Bornot for supporting data management and Lydia Kondyliou for sample management. Joanna Opalinska and Pralay Mukhopadhyay provided clinical development expertise to enable the DREAMM-5 and DREAMM-14 trials. Thank you to all of the patients who took part in the studies and provided permission to collect and use the samples that made these discoveries possible. Editorial support (in the form of writing assistance, including collating and incorporating authors' comments for each draft, assembling tables and figures, grammatical editing and referencing) was provided by Elisabeth Walsby, PhD, CMPP, and Alexus Rivas-John, PharmD, at Fishawack Indicia Ltd, part of Avalere Health, and was funded by GSK.

Authorship contributions

ECRW, UO, SGr were involved in the conception and design of the study, the acquisition of data and the data analysis and interpretation. DEL, SGo, AK, PM, and KR were involved in the design of the study. HAS, MHe, JW, CYW, MHt, LL, VN, WB, BM, RD, PRB, YM, DM, QH, ACA, LL, HCE, EC, YS, JH, FI, GN, and HM were involved in the acquisition of data and data analysis and interpretation. All authors contributed to the writing and reviewing of the manuscript, and have given final approval to the version to be published.

Conflicts of interest

HAS, MHe, JW, HMt, MH, LL, BM, RD, PRB, YM, DM, QH, DEL, DEL, HCE, GN, PL and SGr and AAD are employees of and hold financial equities GSK.

Funding statement

This work was funded by GSK (208887, 209628). The funders of the study had a role in study design, data analysis, data interpretation, and writing of the report.

Data availability

Information about GSK's data sharing commitments can be found at https://www.gsk-studyregister.com/en/.

Additional data may be available from the authors upon reasonable request. For original CyTOF data, please contact edmund.watson@ndorms.ox.ac.uk or udo.oppermann@ndorms.ox.ac.uk; ONT long-read scRNA sequencing data are available at Gene Expression Omnibus (GEO) under accession number GSE307660, Xenium data are available at GEO under accession number GSE307661.

References

1. Keats JJ, Chesi M, Egan JB, et al. Clonal competition with alternating dominance in multiple myeloma. *Blood*. 2012;120(5):1067-1076.
2. Rajkumar SV. Multiple myeloma: 2024 update on diagnosis, risk-stratification, and management. *Am J Hematol*. 2024;99(9):1802-1824.
3. Dhodapkar MV. The immune system in multiple myeloma and precursor states: Lessons and implications for immunotherapy and interception. *Am J Hematol*. 2023;98(S2):S4-S12.
4. Tai Y-T, Mayes PA, Acharya C, et al. Novel anti–B-cell maturation antigen antibody-drug conjugate (GSK2857916) selectively induces killing of multiple myeloma. *Blood*. 2014;123(20):3128-3138.
5. Lonial S, Lee HC, Badros A, et al. Belantamab mafodotin for relapsed or refractory multiple myeloma (DREAMM-2): a two-arm, randomised, open-label, phase 2 study. *The Lancet Oncology*. 2020;21(2):207-221.
6. Watson ECR, Djebbari F, Panitsas F, et al. Belantamab Mafodotin Monotherapy for Multiply-Relapsed Myeloma: A Retrospective Study From the United Kingdom and the Republic of Ireland. *eJHaem*. 2025;6(3):e70039.
7. Hungria V, Robak P, Hus M, et al. Belantamab Mafodotin, Bortezomib, and Dexamethasone for Multiple Myeloma. *N Engl J Med*. 2024;391(5):393-407.
8. Dimopoulos MA, Beksac M, Pour L, et al. Belantamab Mafodotin, Pomalidomide, and Dexamethasone in Multiple Myeloma. *N Engl J Med*. 2024;391(5):408-421.
9. Lonial S, Nooka AK, Thulasi P, et al. Management of belantamab mafodotin-associated corneal events in patients with relapsed or refractory multiple myeloma (RRMM). *Blood Cancer J*. 2021;11(5):103.
10. Montes de Oca R, Alavi AS, Vitali N, et al. Belantamab Mafodotin (GSK2857916) Drives Immunogenic Cell Death and Immune-mediated Antitumor Responses In Vivo. *Mol Cancer Ther*. 2021;20(10):1941-1955.
11. Leong S, Lam HPJ, Kirkham Z, Popat R. Antibody drug conjugates for the treatment of multiple myeloma. *Am J Hematol*. 2023;98(S2):S22-S34.
12. Martins I, Wang Y, Michaud M, et al. Molecular mechanisms of ATP secretion during immunogenic cell death. *Cell Death Differ*. 2014;21(1):79-91.
13. Kroemer G, Galluzzi L, Kepp O, Zitvogel L. Immunogenic Cell Death in Cancer Therapy. *Annu Rev Immunol*. 2013;31(Volume 31, 2013):51-72.
14. Galluzzi L, Vitale I, Warren S, et al. Consensus guidelines for the definition, detection and interpretation of immunogenic cell death. *Journal for ImmunoTherapy of Cancer*. 2020;8(1):e000337.
15. Galluzzi L, Vitale I, Aaronson SA, et al. Molecular mechanisms of cell death: recommendations of the Nomenclature Committee on Cell Death 2018. *Cell Death Differ*. 2018;25(3):486-541.
16. Wittwer NL, Staudacher AH, Liapis V, Cardarelli P, Warren H, Brown MP. An anti-mesothelin targeting antibody drug conjugate induces pyroptosis and ignites antitumor immunity in mouse models of cancer. *J Immunother Cancer*. 2023;11(3).

17. Chen Y, Li X, Yang M, Liu S-B. Research progress on morphology and mechanism of programmed cell death. *Cell Death Dis*. 2024;15(5):327.
18. Tan Y, Chen Q, Li X, et al. Pyroptosis: a new paradigm of cell death for fighting against cancer. *J Exp Clin Cancer Res*. 2021;40(1):153.
19. Ye K, Chen Z, Xu Y. The double-edged functions of necroptosis. *Cell Death Dis*. 2023;14(2):163.
20. Richardson PG, Biswas S, Holkova B, et al. Dreamm-5: Platform Trial Evaluating Belantamab Mafodotin (a BCMA-directed Immuno-conjugate) in Combination with Novel Agents in Relapsed or Refractory Multiple Myeloma (RRMM). *Blood*. 2019;134(Supplement_1):1857-1857.
21. Love M, Huber W, Anders S. Moderated estimation of fold change and dispersion for RNA-seq data with DESeq2. *Genome Biol*. 2014;15(12):550.
22. Stephens M. False discovery rates: a new deal. *Biostatistics*. 2017;18(2):275-294.
23. Ignatiadis N, Klaus B, Zaugg JB, Huber W. Data-driven hypothesis weighting increases detection power in genome-scale multiple testing. *Nat Methods*. 2016;13(7):577-580.
24. Wolf FA, Angerer P, Theis FJ. SCANPY: large-scale single-cell gene expression data analysis. *Genome Biol*. 2018;19(1):15.
25. Young MD, Behjati S. SoupX removes ambient RNA contamination from droplet-based single-cell RNA sequencing data. *GigaScience*. 2020;9(12).
26. Germain P-L, Lun Aaron TL, Garcia Meixide C, Macnair W, Robinson MD. Doublet identification in single-cell sequencing data using scDblFinder. *F1000Research*. 2022; 10.
27. Gayoso A, Lopez R, Xing G, et al. A Python library for probabilistic analysis of single-cell omics data. *Nat Biotechnol*. 2022;40(2):163-166.
28. Hao Y, Hao S, Andersen-Nissen E, et al. Integrated analysis of multimodal single-cell data. *Cell*. 2021;184(13):3573-3587.e3529.
29. Jin S, Plikus MV, Nie Q. CellChat for systematic analysis of cell–cell communication from single-cell transcriptomics. *Nat Protoc*. 2025;20(1):180-219.
30. Yu P, Zhang X, Liu N, Tang L, Peng C, Chen X. Pyroptosis: mechanisms and diseases. *Signal Transduct Target Ther*. 2021;6(1):128.
31. Hultcrantz M, Kleinman D, Ghataorhe P, et al. PB2022: Exploring alternative dosing regimens of single-agent belantamab mafodotin on safety and efficacy in patients with relapsed or refractory multiple myeloma: DREAMM-14. *HemaSphere*. 2022;6:1893-1894.
32. Acharya N, Sabatos-Peyton C, Anderson AC. Tim-3 finds its place in the cancer immunotherapy landscape. *J Immunother Cancer*. 2020;8(1).
33. Hájek R, Jungova A, Minarik J, et al. Clinical Unmet Need of Lenalidomide-Refractory vs Non-Lenalidomife-Refractory Patients With Multiple Myeloma in the Honeur Federated Data Network. Abstract and poster # PS1745. EHA. Milan, Italy; 2025.
34. Kostopoulos IV, Kakalis A, Birmpilis A, et al. Belantamab mafodotin induces immunogenic cell death within 24 h post-administration in newly diagnosed multiple myeloma patients. *Am J Hematol*. 2023;98(3):E65-E67.
35. Hughes CE, Nibbs RJB. A guide to chemokines and their receptors. *The FEBS Journal*. 2018;285(16):2944-2971.
36. Ben-Sasson SZ, Wang K, Cohen J, Paul WE. IL-1β Strikingly Enhances Antigen-Driven CD4 and CD8 T-Cell Responses. *Cold Spring Harb Symp Quant Biol*. 2013;78:117-124.

37. Yatim N, Jusforgues-Saklani H, Orozco S, et al. RIPK1 and NF-κB signaling in dying cells determines cross-priming of CD8⁺ T cells. *Science*. 2015;350(6258):328-334.
38. Bronte V, Brandau S, Chen S-H, et al. Recommendations for myeloid-derived suppressor cell nomenclature and characterization standards. *Nature Communications*. 2016;7(1):12150.
39. Kim S, Kwak J-E, Koh J-Y, et al. CD4 Cytotoxic T Cells Promote Antitumor Immunity in Multiple Myeloma. *Blood*. 2024;144(Supplement 1):668-668.
40. Preglej T, Ellmeier W. CD4+ Cytotoxic T cells – Phenotype, Function and Transcriptional Networks Controlling Their Differentiation Pathways. *Immunol Lett*. 2022;247:27-42.

Figure Legends

Figure 1. Belantamab mafodotin triggers hallmarks of ICD and inflammatory cell death in NCI-H929 and primary MM cells

Percentage of NCI-H929 cells expressing distinct markers of ICD at the cell surface as measured by spectral flow cytometry after 72 hours of treatment with various concentrations of belantamab mafodotin (belamaf) or IgG1 as a negative control (A) or free-MMAF with DMSO as a negative control (B). (C–D) MA plot of RNAseq results of belantamab mafodotin 10 µg/mL vs IgG control showing mean log2 expression on x-axis and moderated log2 fold change on y-axis. FDR was controlled using Independent Hypothesis Weighting, with genes meeting the significance threshold (FDR < 0.1) are shown in green. Genes implicated in cell death pathways are highlighted in red for necroptosis (C) and pyroptosis (D). (E–F) Primary patient BMMCs were incubated with belantamab mafodotin for 16 hours and cell surface markers were assessed by spectral flow cytometry. For each marker, a binomial proportions model was used to compare treatment response vs IgG1 vehicle control and the BH multiplicity correction was applied to control the FDR set at 5%. Graphs represent an exemplar plot from an individual donor (E) and amalgamated data from all 7 donors where the colours represent donors and the dots represent replicates (F). Error bars are standard error of the mean, ***P<0.001; **P<0.01; *P<0.05. Belamaf, belantamab mafodotin.

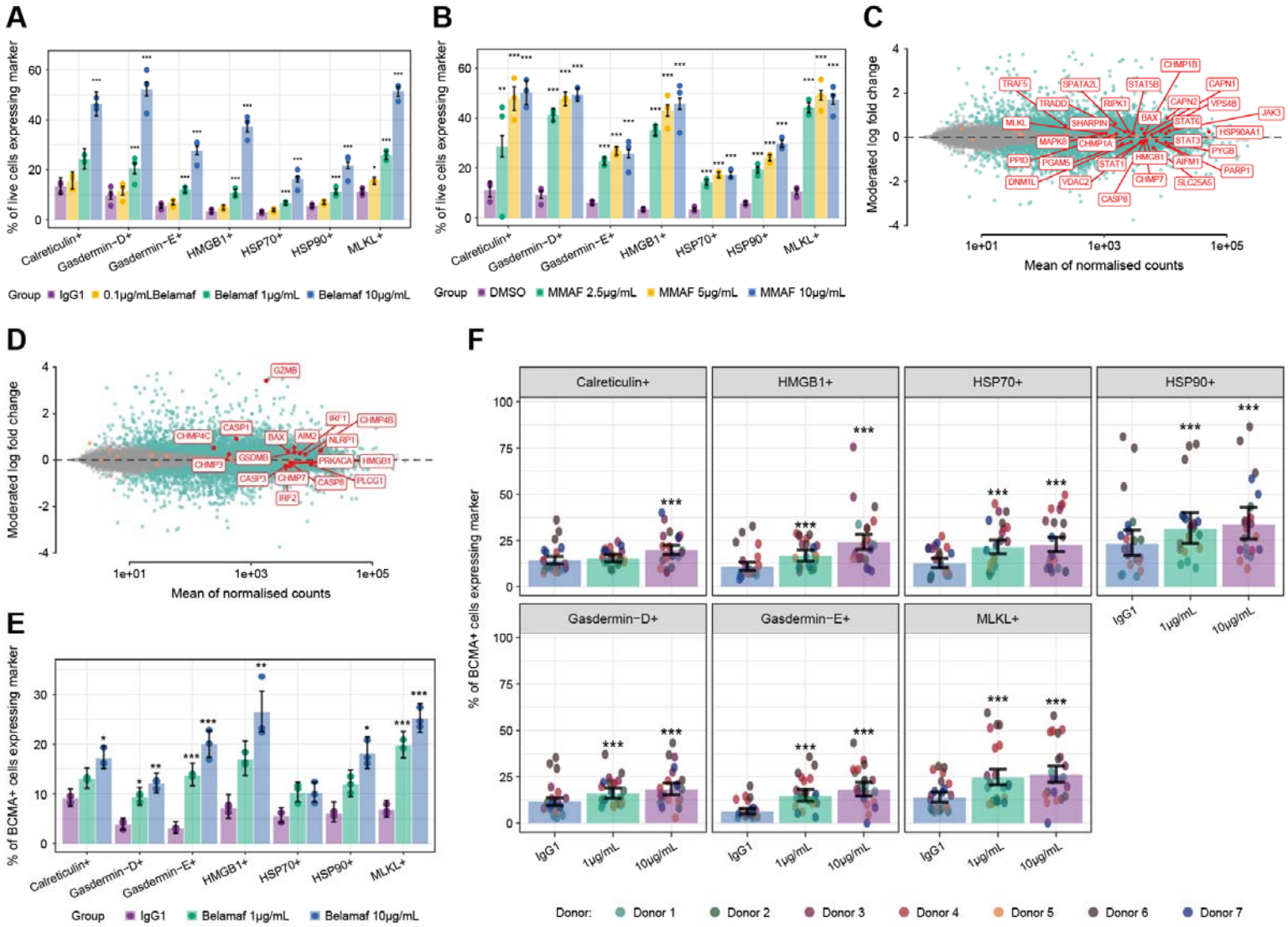
A
% of live cells expressing marker
Calreticulin+
Gasdermin-D+
Gasdermin-E+
HMGB1+
HSP70+
HSP90+
MLKL+
Group IgG1 0.1μg/mLBelamaf Belamaf 1μg/mL Belamaf 10μg/mL
B
% of live cells expressing marker
Group DMSO MMAF 2.5μg/mL MMAF 5μg/mL MMAF 10μg/mL
C
Moderated log fold change
Mean of normalised counts
D
Moderated log fold change
Mean of normalised counts
E
% of BCMA+ cells expressing marker
Group IgG1 Belamaf 1μg/mL Belamaf 10μg/mL
F
% of BCMA+ cells expressing marker
Calreticulin+
HMGB1+
HSP70+
HSP90+
Gasdermin-D+
Gasdermin-E+
MLKL+
IgG1
1μg/mL
10μg/mL
Donor: Donor 1 Donor 2 Donor 3 Donor 4 Donor 5 Donor 6 Donor 7

Figure 2. Soluble markers of inflammatory and immunogenic cell death are enriched in the supernatant of belantamab mafodotin-treated NCI-H929 and primary MM cells

(A) Volcano plots visualizing the Log2 fold changes in analyte concentrations in the supernatant from NCI-H929 cells treated for 48 and 72 hours with belantamab mafodotin (belamaf) at 0.1, 1, and 10 µg/mL. Proteins showing a Log2 fold change of at least 1 and an adjusted P-value of <0.05 are considered significantly modulated and are colored in red. Selected significant proteins are indicated by gene name. (B) Heatmap comparing transcript changes (RNAseq, moderated LFC) with secreted protein levels in supernatants from belantamab mafodotin-treated cells (Olink, LFC) for CCL3, CCL4, CXCL8, and GZMB. n.s. = not significant (FDR > 0.05). (C) Concentration of selected pro-inflammatory molecules in the supernatant of NCI-H929 cells treated with belantamab mafodotin as measured by MSD. Dotted line indicates lower limit of detection (LOD) of the assay in the linear range. Error bars are standard error of the mean. (D) Concentration of the same molecules in the supernatant of belantamab mafodotin-treated primary patient cells. Dotted lines indicate lower limit of detection of the assay in the linear range. Error bars are standard error of the mean. For each of the secreted inflammatory mediators, a Bayesian Tobit model was implemented to compare treatment vs IgG control. ***P<0.001; **P<0.01; *P<0.05. Belamaf, belantamab mafodotin.

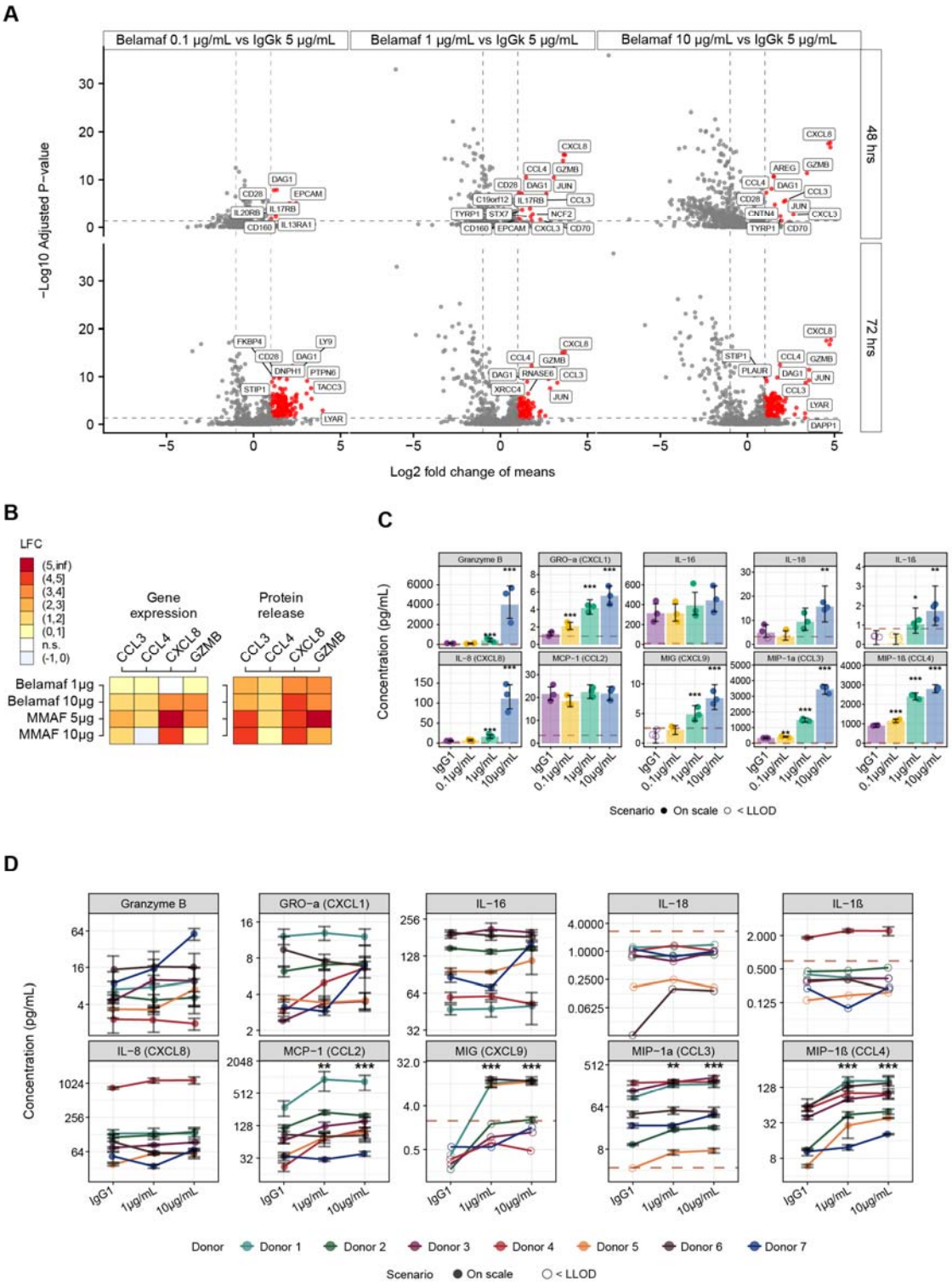
A
Belamaf 0.1 µg/mL vs IgGk 5 µg/mL
Belamaf 1 µg/mL vs IgGk 5 µg/mL
Belamaf 10 µg/mL vs IgGk 5 µg/mL
48 hrs
72 hrs
−Log10 Adjusted P−value
Log2 fold change of means
B
LFC
(5,inf)
(4,5]
(3,4]
(2,3]
(1,2]
(0,1]
n.s.
(-1,0)
Gene expression
Protein release
CCL3
CCL4
CXCL8
GZMB
Belamaf 1µg
Belamaf 10µg
MMAF 5µg
MMAF 10µg
C
Granzyme B
GRO−a (CXCL1)
IL−16
IL−18
IL−1ß
IL−8 (CXCL8)
MCP−1 (CCL2)
MIG (CXCL9)
MIP−1a (CCL3)
MIP−1ß (CCL4)
Concentration (pg/mL)
IgG1
0.1µg/mL
1µg/mL
10µg/mL
Scenario ● On scale ○ < LLOD
D
Donor
Donor 1
Donor 2
Donor 3
Donor 4
Donor 5
Donor 6
Donor 7
Scenario ● On scale ○ < LLOD

Figure 3. Belantamab mafodotin triggers hallmarks of acute, transient inflammation in patient serum

Concentration of inflammatory mediators in serum samples from 43 patients in DREAMM-14 treated with various dosing regimens of belantamab mafodotin monotherapy. Serum samples were collected at three time points for each patient: Dose 1 – Predose; 24 hours post-dose 1; and prior to Dose 2. Statistical analysis was conducted using a Bayesian Tobit models (for HMGB1 and IL1β markers) or a Linear Mixed-effect Models (LMM) for the remaining markers. The p-values for pairwise comparisons of the three time points obtained from the LMM have been adjusted using the Tukey-Kramer method (A) Quantification of the ICD marker HMGB1 by ELISA. (B) Comparative concentrations of secreted IL8, Granzyme B, IL16, CCL3, CCL4, IL18, IL1β, CXCL9, CCL2, and CXCL1 quantified using the MSD 10-plex assay across different dosing regimens.

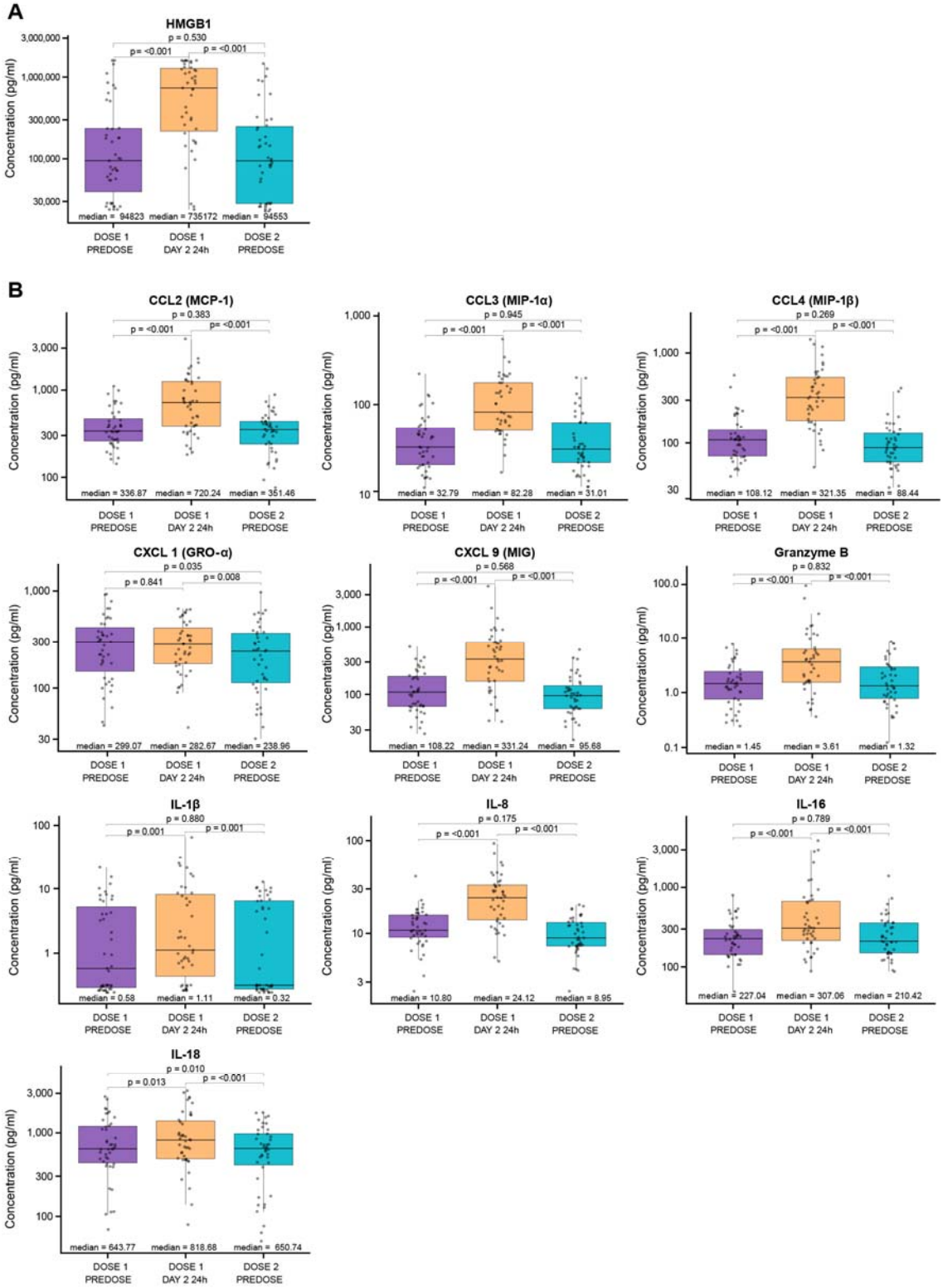
A
HMGB1
p = 0.530
p = <0.001
p = <0.001
Concentration (pg/ml)
3,000,000
1,000,000
300,000
100,000
30,000
median = 94823
median = 735172
median = 94553
DOSE 1 PREDOSE
DOSE 1 DAY 2 24h
DOSE 2 PREDOSE
B
CCL2 (MCP-1)
p = 0.383
p = <0.001
p = <0.001
median = 336.87
median = 720.24
median = 351.46
CCL3 (MIP-1α)
p = 0.945
p = <0.001
p = <0.001
median = 32.79
median = 82.28
median = 31.01
CCL4 (MIP-1β)
p = 0.269
p = <0.001
p = <0.001
median = 108.12
median = 321.35
median = 88.44
CXCL 1 (GRO-α)
p = 0.035
p = 0.841
p = 0.008
median = 299.07
median = 282.67
median = 238.96
CXCL 9 (MIG)
p = 0.568
p = <0.001
p = <0.001
median = 108.22
median = 331.24
median = 95.68
Granzyme B
p = 0.832
p = <0.001
p = <0.001
median = 1.45
median = 3.61
median = 1.32
IL-1β
p = 0.880
p = 0.001
p = 0.001
median = 0.58
median = 1.11
median = 0.32
IL-8
p = 0.175
p = <0.001
p = <0.001
median = 10.80
median = 24.12
median = 8.95
IL-16
p = 0.789
p = <0.001
p = <0.001
median = 227.04
median = 307.06
median = 210.42
IL-18
p = 0.010
p = 0.013
p = <0.001
median = 643.77
median = 818.68
median = 650.74

Figure 4. A subset of inflammatory chemokines was associated with the depth of response in patients

Concentration of inflammatory mediators (A) CCL4, (B) CXCL9, (C) CCL3 and (D) Granzyme B in serum samples from patients in DREAMM-14 treated with belantamab mafodotin monotherapy. Serum samples were collected at three time points for each patient: Dose 1 – Predose; Dose 1 – 24 hours post-dose; and Dose 2 – Predose. Data are grouped by patient response. Deep responder = patients who achieved a very good partial response (VGPR), complete response (CR), or stringent complete response (sCR). Modest responders = patients who achieved a partial response (PR), minimal response (MR), or stable disease (SD). Non-responders = progressive disease (PD). LMM was used to evaluate if the longitudinal profile of a marker differed by response categories. The overall difference is characterized by the "interaction P-value" which has been adjusted for multiple testing of the 9 markers using the Benjamini-Hochberg FDR method. For pairwise comparisons between three time points within response groups, the p-values have been adjusted using the Tukey-Kramer method.

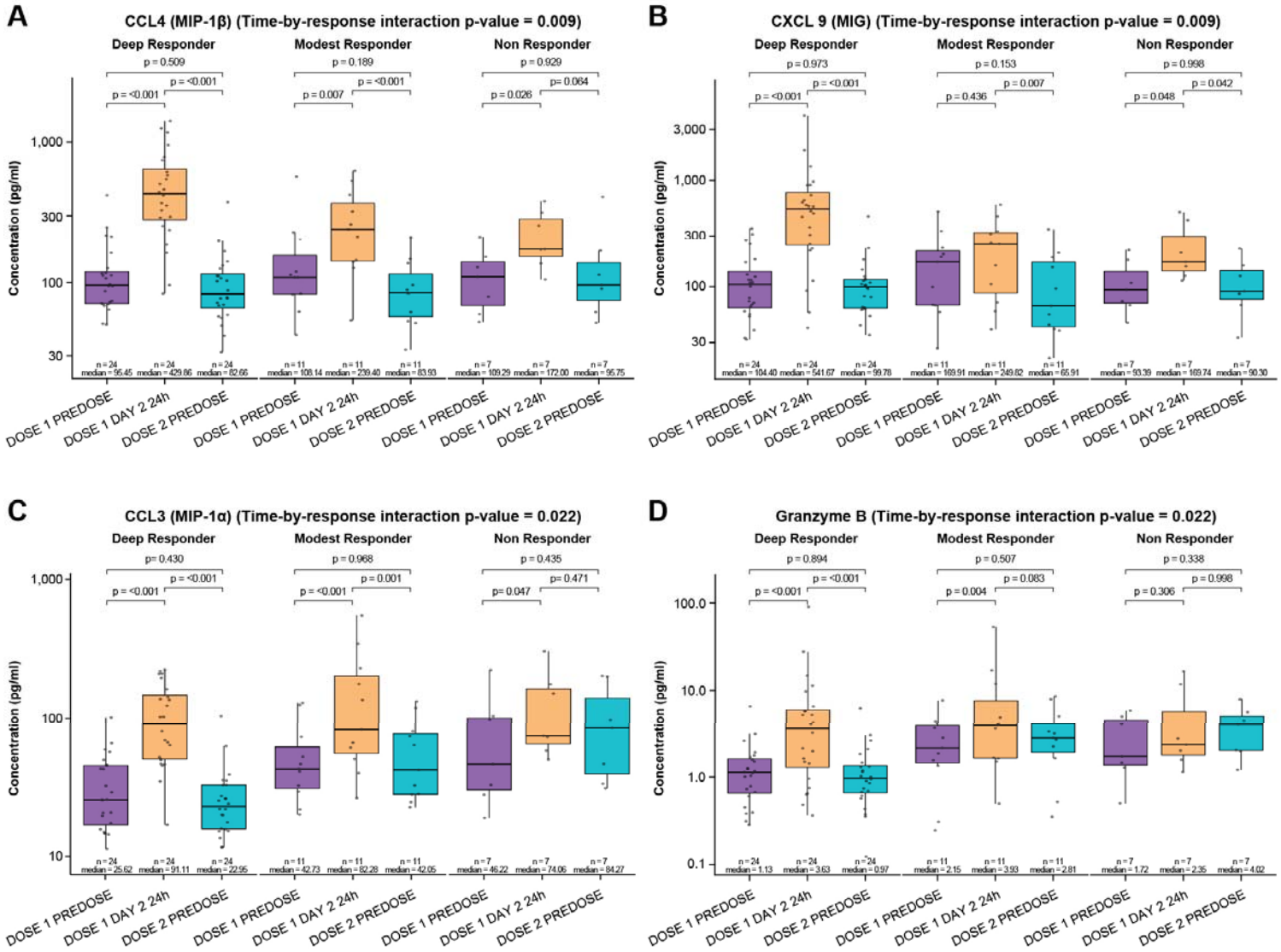
A
CCL4 (MIP-1β) (Time-by-response interaction p-value = 0.009)
Deep Responder
Modest Responder
Non Responder
Concentration (pg/ml)
DOSE 1 PREDOSE
DOSE 1 DAY 2 24h
DOSE 2 PREDOSE
B
CXCL 9 (MIG) (Time-by-response interaction p-value = 0.009)
C
CCL3 (MIP-1α) (Time-by-response interaction p-value = 0.022)
D
Granzyme B (Time-by-response interaction p-value = 0.022)

Figure 5. Monocytoid cells are a dominant cell type in the MM TME and are equipped to respond to ICD

(A) UMAP dimensionality reduction of long read scRNAseq data from patient samples (15 samples total, across 12 separate patients) plus 4 control samples, integrated by scVI and colored by cell type. (B) Neighbourhood analysis of pre-treatment patient samples compared with control samples, plotted in the same UMAP axes as (A), where blue shading in the circles means increased in patient samples and red means increased in control samples. Size of circles proportionate to size of neighborhoods, and thickness of edges related to connectivity of neighborhoods. (C) Beeswarm plot showing differential abundance of cell types as determined by scRNAseq in pre-treatment patient samples vs control; as with (C), more negative numbers suggest more abundant in controls, more positive numbers indicate more abundant in patients. Each point represents a neighbourhood, which are coloured if they are significantly differentially abundant at an FDR of 0.1. (D) Violin plots of scRNAseq data showing relative expression of key immunogenic and inflammatory receptors in monocytoid and cDC populations, grouped according to ligand; long read scRNAseq data. Pseudobulk analysis using DESeq2 method for differential expression. Multiple hypothesis testing adjusted for by Benjamini-Hochberg method, where P-adjusted values for comparisons are * $P<0.05$, ** $P<0.005$, *** $P<0.0005$. Only the receptors with significant results are shown. (E–F) Beeswarm plots of mass cytometry data of the same MM baseline samples, showing differences in the monocytoid (E) and classical dendritic cell (cDC) (F) populations in responding vs non-responding patients at baseline. Positive values represent over-representation in responders. Non-paired analysis, performed with MiloR, where colored dots refer to statistically significant events at the FDR value of 0.2.

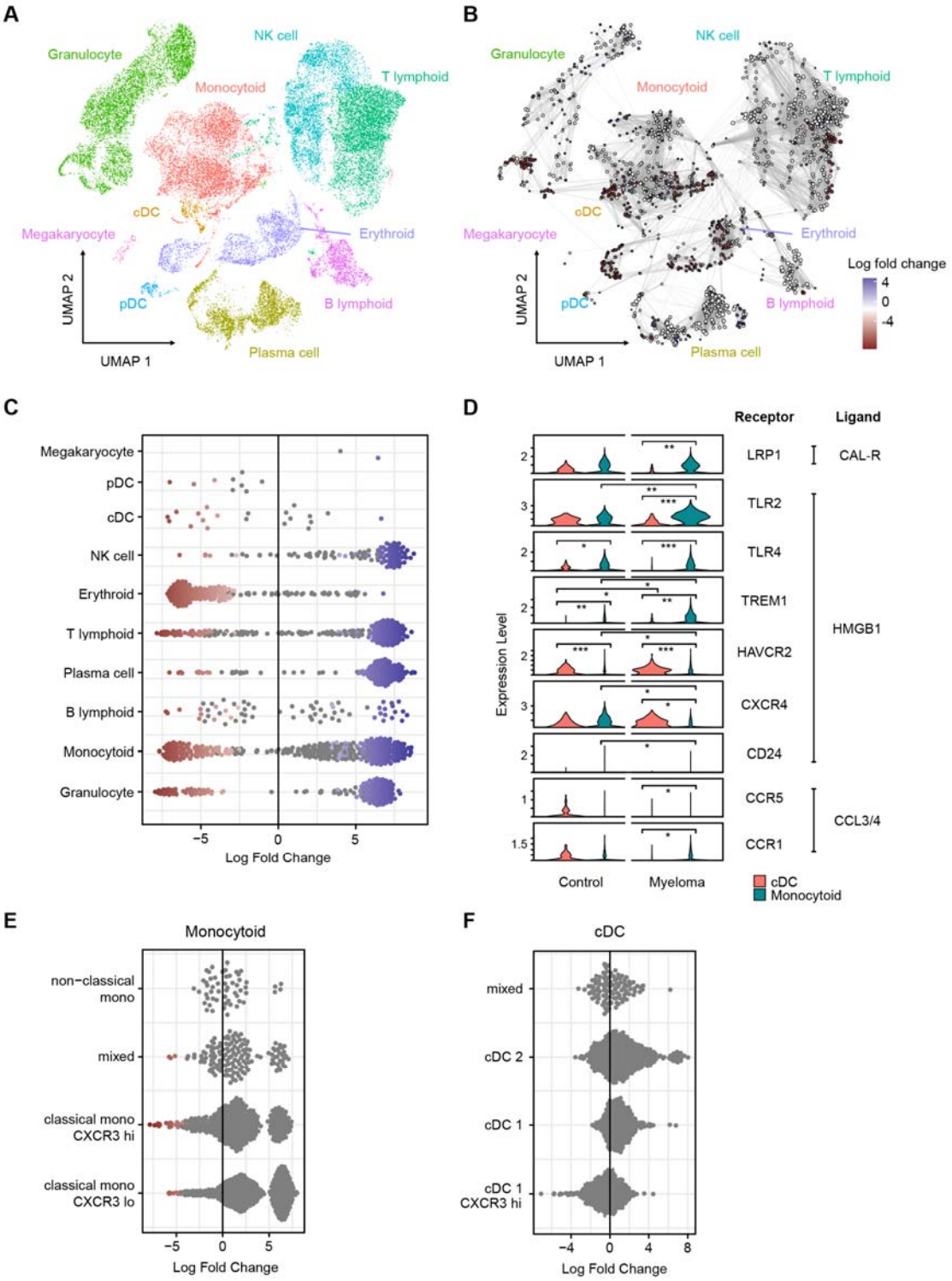
A
Granulocyte
NK cell
T lymphoid
Monocytoid
cDC
Megakaryocyte
Erythroid
pDC
B lymphoid
Plasma cell
UMAP 2
UMAP 1
B
Log fold change
4
0
-4
C
Megakaryocyte
pDC
cDC
NK cell
Erythroid
T lymphoid
Plasma cell
B lymphoid
Monocytoid
Granulocyte
−5
0
5
Log Fold Change
D
Receptor
Ligand
LRP1
CAL-R
TLR2
TLR4
TREM1
HAVCR2
CXCR4
CD24
HMGB1
CCR5
CCR1
CCL3/4
Expression Level
Control
Myeloma
cDC
Monocytoid
E
Monocytoid
non−classical mono
mixed
classical mono CXCR3 hi
classical mono CXCR3 lo
−5
0
5
Log Fold Change
F
cDC
mixed
cDC 2
cDC 1
cDC 1 CXCR3 hi
−4
0
4
8
Log Fold Change

Figure 6. The BM of responding patients shows signs of invigoration and emergence of adaptive immunity

Single cell *in situ* spatial transcriptomics was performed on three MM BM trephines **(see Supplemental Figure 4)**. (A) UMAP plots of integrated spatial transcriptomic data from selected tiles across 3 patient samples: patient MM075 baseline (top); patient MM075 remission (middle); patient MM263 relapse (bottom). (B) Violin plot of selected immune checkpoint and exhaustion markers, reflecting expression levels in tiles selected for analysis. Statistical comparisons were performed using Seurat FindMarkers with t-test as test model. Significance is indicated as follows: BH-adjusted P<0.05 (*), P<0.005 (**), P<0.0005 (***). (C–H) Mass cytometry data from full monotherapy cohort. (C–D) Beeswarm plots of granulocytes showing changes in cellular neighbourhoods in responders vs non-responders at baseline (C) (where positive values represent over-representation in responders) and in baseline vs follow-up in responders (D) (where positive values represent over-expression at follow-up). (E) UMAP of mass cytometry data of T-lymphoid cells only. (F–G) Beeswarm plots of T cells analyzed as per granulocytes, comparing responders vs non-responders at baseline (F) and baseline vs follow-up in responders (G). (H) CD4 GZMB high cells and CD8 NKG2A high cells analyzed at follow-up, where more positive values indicate greater abundance in the remission state. All beeswarm plots produced by non-paired analysis in MiloR, with neighborhoods shaded if significant at an FDR of 0.2.

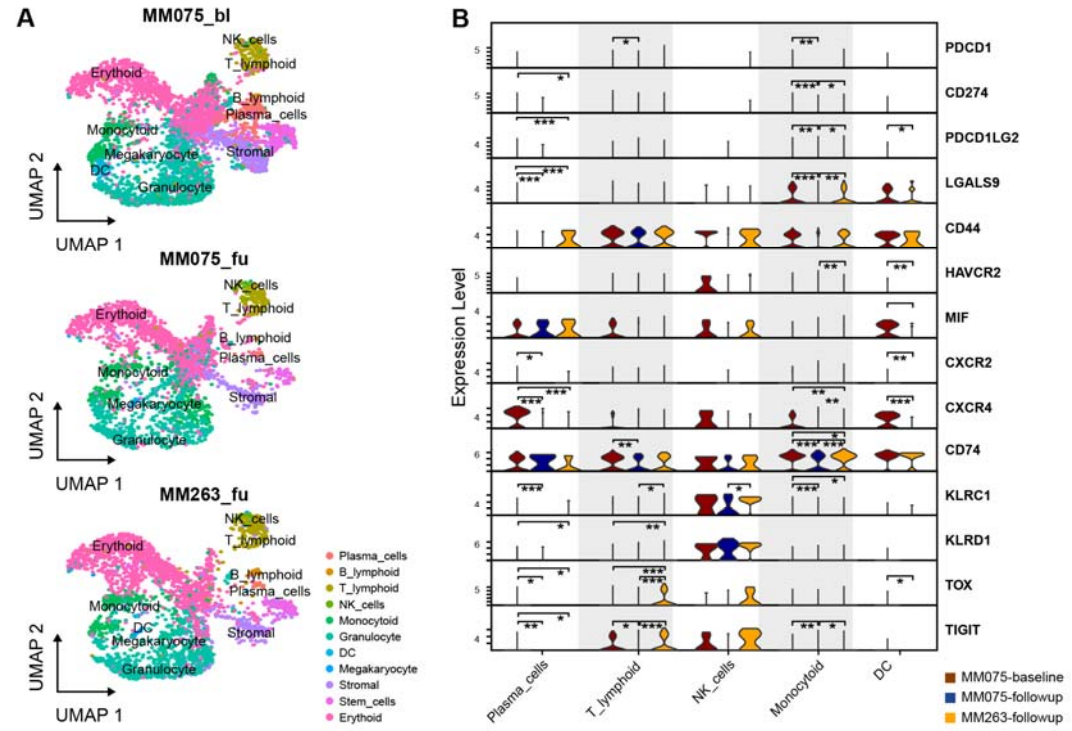
A
MM075_bl
NK_cells
T_lymphoid
Erythoid
B_lymphoid
Plasma_cells
Monocytoid
Megakaryocyte
Stromal
DC
Granulocyte
UMAP 2
UMAP 1
MM075_fu
MM263_fu
Plasma_cells
B_lymphoid
T_lymphoid
NK_cells
Monocytoid
Granulocyte
DC
Megakaryocyte
Stromal
Stem_cells
Erythoid
B
Expression Level
PDCD1
CD274
PDCD1LG2
LGALS9
CD44
HAVCR2
MIF
CXCR2
CXCR4
CD74
KLRC1
KLRD1
TOX
TIGIT
Plasma_cells
T_lymphoid
NK_cells
Monocytoid
DC
MM075-baseline
MM075-followup
MM263-followup

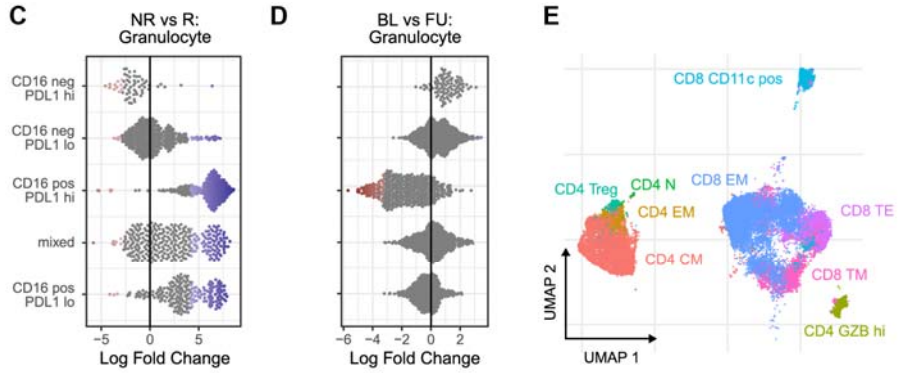
C
NR vs R:
Granulocyte
CD16 neg PDL1 hi
CD16 neg PDL1 lo
CD16 pos PDL1 hi
mixed
CD16 pos PDL1 lo
Log Fold Change
D
BL vs FU:
Granulocyte
Log Fold Change
E
CD8 CD11c pos
CD4 Treg
CD4 N
CD8 EM
CD4 EM
CD8 TE
CD4 CM
CD8 TM
CD4 GZB hi
UMAP 2
UMAP 1

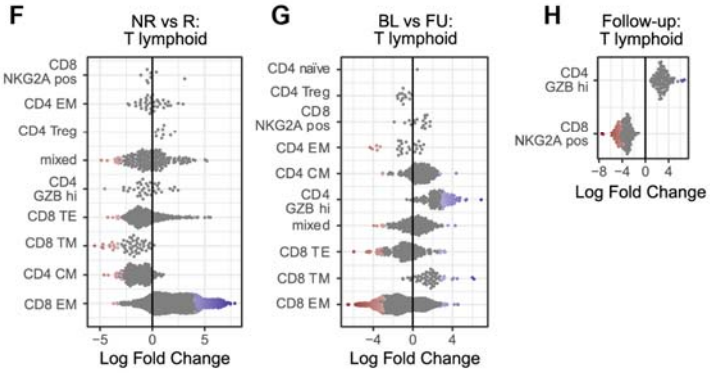
F
NR vs R:
T lymphoid
CD8 NKG2A pos
CD4 EM
CD4 Treg
mixed
CD4 GZB hi
CD8 TE
CD8 TM
CD4 CM
CD8 EM
Log Fold Change
G
BL vs FU:
T lymphoid
CD4 naïve
CD4 Treg
CD8 NKG2A pos
CD4 EM
CD4 CM
CD4 GZB hi
mixed
CD8 TE
CD8 TM
CD8 EM
Log Fold Change
H
Follow-up:
T lymphoid
CD4 GZB hi
CD8 NKG2A pos
Log Fold Change